

Electrochemistry of Aqueous Pyridinium: Exploration of A Key Aspect of Electrocatalytic Reduction of CO₂ to Methanol

Yong Yan, Elizabeth L. Zeitler, Jing Gu, Yuan Hu and Andrew B. Bocarsly*

Department of Chemistry, Princeton University, Princeton, New Jersey 08544

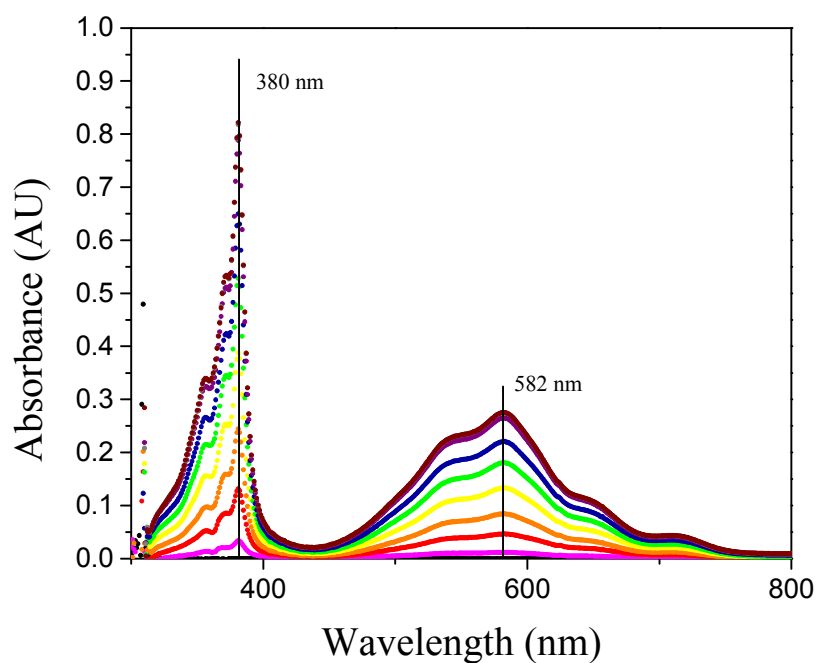


Figure S1. Electrochemical generation of 4,4'-bipyridinium radical at -0.9 V vs. SCE on a platinum electrode as observed spectroelectrochemically. UV-visible spectra were recorded over 680 seconds and showed growth in of the radical spectrum¹ with maxima at 380 nm and 582 nm during continued electrolysis.

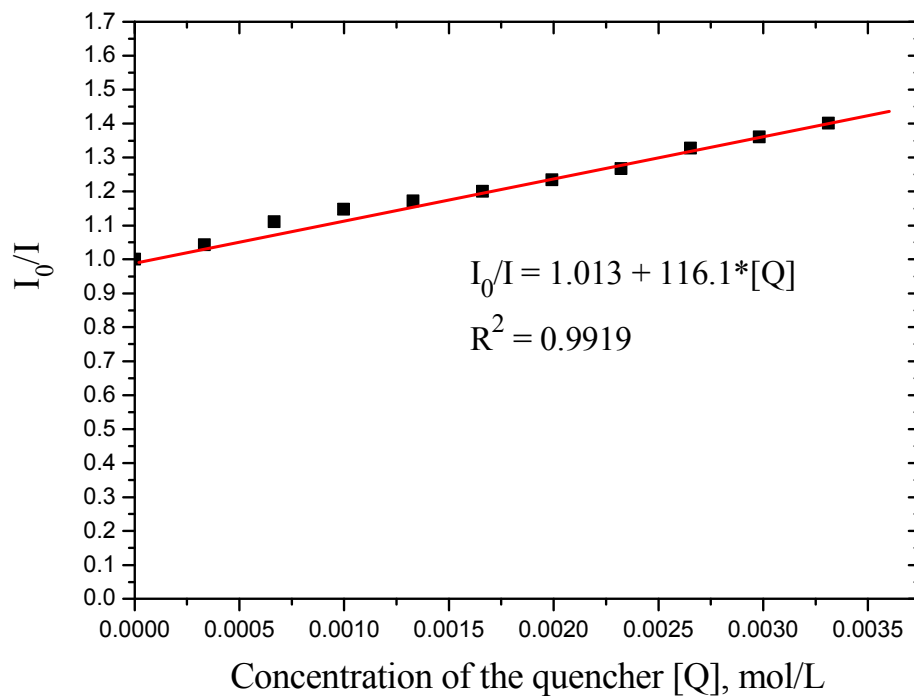


Figure S2. Stern-Volmer charge transfer quenching of excited $[\text{Ir}(\text{ppy})_3]$ by pyridinium. The quenching rate constant, k_q , was obtained from:

$$I_0/I = 1 + K_{sv}[Q];$$

$$K_{sv} = k_q \times \tau \quad (\tau = 1.9 \mu\text{s}).$$

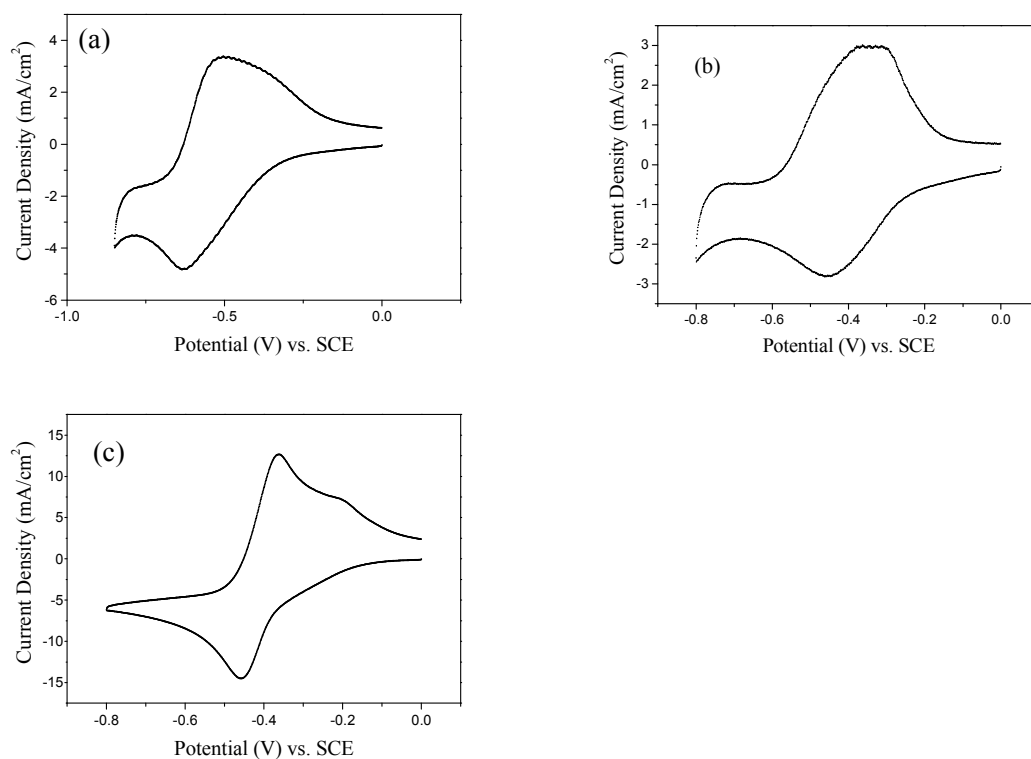
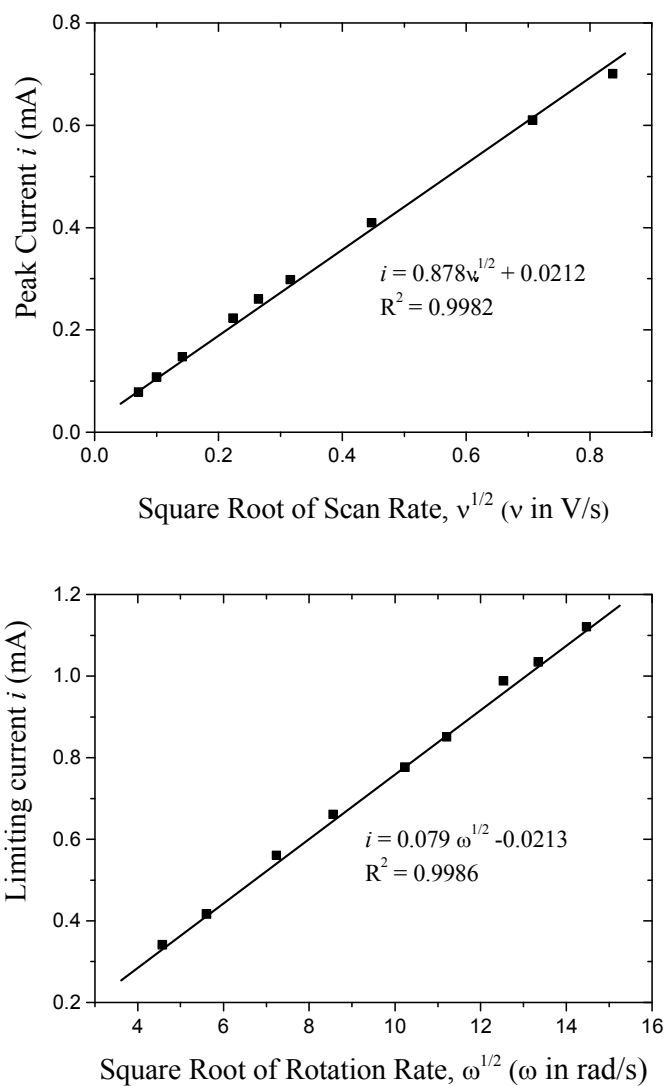


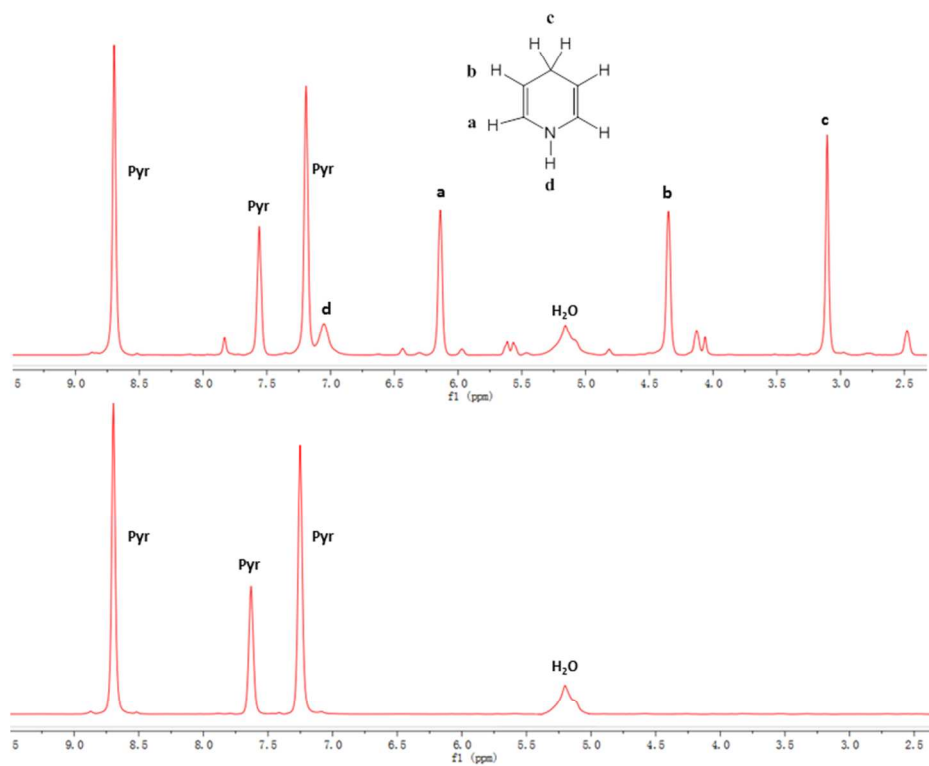
Figure S3. Comparison of cyclic voltammetry of pyridinium (a), acetic acid (b) and H₃O⁺ (c) all at 5 mM concentration on a platinum electrode at 1000 mV/s. Prefeatures at more positive potentials than the diffusion limited wave were observed in cyclic voltammograms of all these species at the selected scan rate.



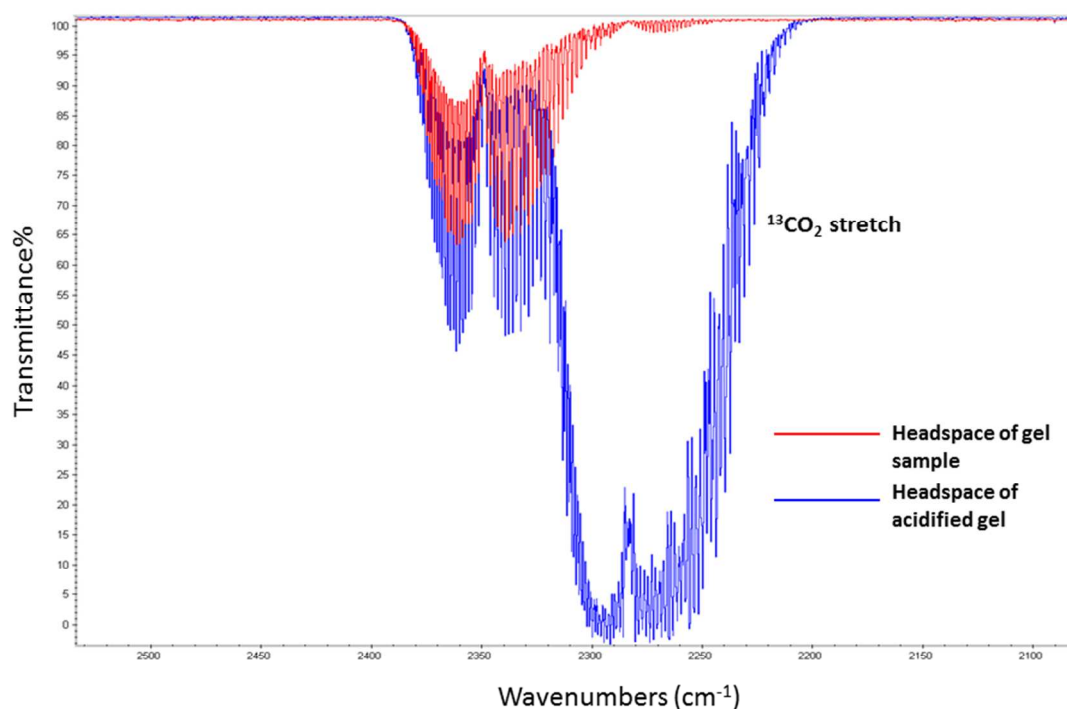
$$i_p = 2.69 \times 10^5 n^{3/2} A C_o^* D^{1/2} v^{1/2} \quad (1)$$

$$i_l = 0.62 n F A C_o^* D^{2/3} v^{-1/6} \omega^{1/2} \quad (2)$$

Figure S4. Cyclic voltammetric scan rate dependence (top) and rotating disk voltammetric rotation rate dependence (bottom) of pyridinium reduction at a platinum electrode at pH = 5.2, showing linearity and slopes used to calculate n and D . Equation 1 relates peak current for a reversible couple in a cyclic voltammogram at 25 °C, with i_p in amperes, $A = 0.196 \text{ cm}^2$, D in $\text{cm}^2 \text{ s}^{-1}$, $C_o^* = 5.0 \times 10^{-6} \text{ mol cm}^{-2}$ and v in V s^{-1} . Equation 2 expresses the Levich limiting current for a reversible couple in rotating disk voltammetry at 25 °C, with current in amperes, F , the Faraday constant = $96,485 \text{ C mol}^{-1}$, $A = 0.196 \text{ cm}^2$, $C_o^* = 5.0 \times 10^{-6} \text{ mol cm}^{-2}$, D in $\text{cm}^2 \text{ s}^{-1}$, $v = 0.008823 \text{ cm}^2 \text{ s}^{-1}$ in and ω in rad s^{-1} .



(a)



(b)

Figure S5. (a) Free 1,4-dihydropyridine was observed in the upper ^1H NMR spectrum collected from hydrolyzed lithium tetrakis(N-dihydropyridyl) aluminate in deuterated pyridine. A small amount of unlabeled 1,2-DHP was also observed. After bubbling CO_2 into the NMR tube, which formed a gel, the lower spectrum was collected. All the DHP peaks disappeared as the gel formed, but no reduced CO_2 products were detected. (b) The Ar purged headspace of a NMR tube containing gel formed by reacting $^{13}\text{CO}_2$ with the DHP was collected. The (red) gas phase IR spectrum of this sample showed only $^{12}\text{CO}_2$ stretches from unlabeled environmental CO_2 and no ^{13}C products. When acidified with concentrated HCl the gel dissociated and bubbles were released into the headspace, resulting in the observation of $^{13}\text{CO}_2$ stretches in the range $2225 - 2350\text{ cm}^{-1}$ (blue). This set of experiments unambiguously demonstrated that DHP does not react with CO_2 in homogenous solution to form reduced products.

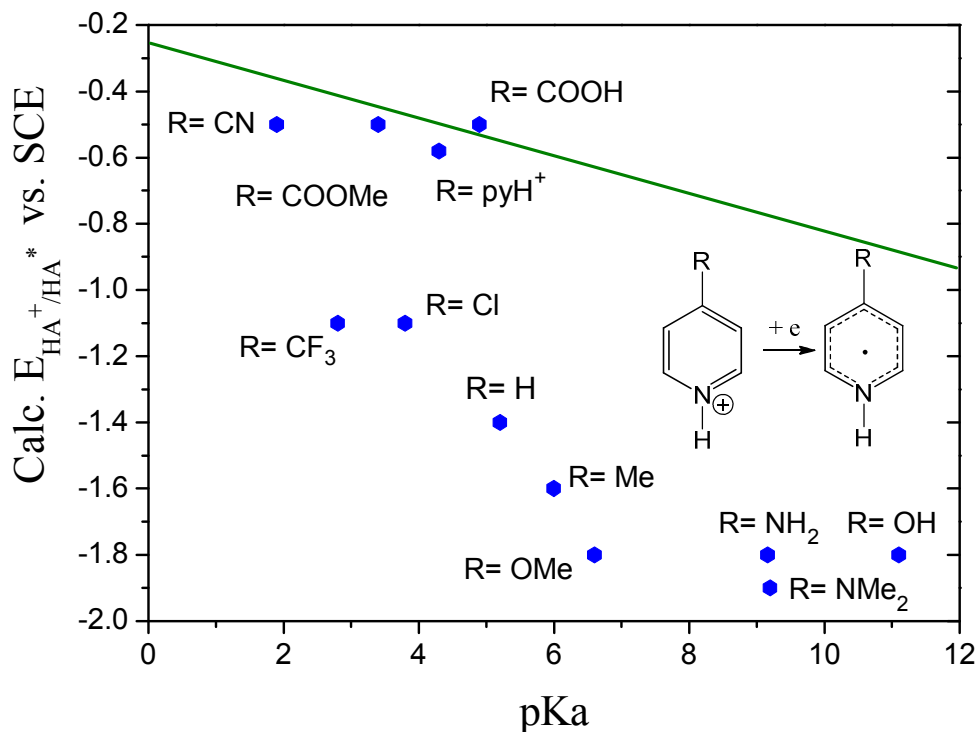


Figure S6. Calculated π -orbital based standard reduction potentials based on Keith and Carter's methodology, E_{HA^+/HA^\bullet} (dots), compared to the weak acid based, proton reduction trend line for various pyridinium derivatives. Obviously, the π -based redox potential does not correlate with pK_a value, but rather qualitatively relates to the electron donor ability as well as π -orbital conjugation/delocalization. The position of the calculated redox potentials of the compounds relative to the weak acid reduction trend indicates what type of reduction is energetically preferred. Those compounds with reduction potentials located more negative than the weak acid reduction trend line prefer to reduce via the energetically more favorable proton reduction, while those with calculated potentials above the line would prefer to reduce via the π -orbital mechanism. Both pathways may compete for those compounds with calculated π -orbital reduction potentials located near to the proton reduction trend. In general, for the acids surveyed, most of pyridinium derivatives would π -reduce more negative than the weak acid trend.

Table S-1. Weak acids studied in this work along with their pK_a ^{2,3} and observed reduction potential on a platinum electrode.

Weak Acids	pK_a	$E_{1/2}$	Weak Acids	pK_a	$E_{1/2}$
Et₃NH⁺	10.7	-0.92	4-methylpyridinium	6.0	-0.64
C₆H₅OH	10.0	-0.87	4-tertbutylpyridinium	6.0	-0.64
NH₄⁺	9.2	-0.83	3-methyl pyridinium	5.7	-0.62
m-NO₂C₆H₄OH	8.4	-0.79	benzimidazolium	5.6	-0.61
morpholinium	8.3	-0.78	pyridinium	5.2	-0.58
N-Methyl morpholinium	7.4	-0.72	3-methoxypyridinium	4.9	-0.56
1-methyl imidazolium	7.4	-0.72	acetic acid	4.7	-0.55
p-NO₂C₆H₄OH	7.1	-0.7	anilinium	4.6	-0.54
imidazolium	7.0	-0.7	3-methoxylanilinium	4.2	-0.52
2,6-lutidinium	6.7	-0.68	benzoic acid	4.2	-0.52
p-NO₂C₆H₄OH	7.1	-0.7	formic acid	3.8	-0.49
3,4-lutidinium	6.5	-0.67	Ethyl isonicotinate	3.5	-0.47

References:

- (1) Brateman, P. S.; Song, J. I. *The Journal of Organic Chemistry* **1991**, *56*, 4678.
- (2) In *CRC Handbook of Chemistry and Physics*; Haynes, W. M., Ed.; CRC Press/Taylor and Francis: Boca Raton, FL, 2011.
- (3) Tenenbaum, L. E. In *The Chemistry of Heterocyclic Compounds, Pyridine and its Derivatives*; Klingsberg, E., Ed.; John Wiley and Sons: New York, 1961; Vol. 14/2, p 176.